Improvement in the digital acquisition of the pupillary response to controlled stimulation by means of computational tools and low-cost optoelectronics device

M. S. GOMEZ-DIAZ[1], D. A. GUTIÉRREZ-HERNANDEZ[2], F. J. CASILLAS-RODRIGUEZ[1,*], M. MORA-GONZALEZ[1], C. I. MEDEL-RUIZ[1], J. MUÑOZ-MACIEL[1]
[1]*Universidad de Guadalajara, Centro Universitario de los Lagos, Av. Enrique Díaz de León No. 1144, Colonia Paseos de la Montaña C.P. 47460, Lagos de Moreno, Jalisco, México*
[2]*Tecnológico Nacional de México. Instituto Tecnológico de León. División de Estudios de Posgrado e Investigación. Avenida Tecnológico s/n, Industrial Julián de Obregón, C.P. 37290 León, Guanajuato, México*

There are various electronic devices developed with state-of-the-art technology, which can be used inside and outside a hospital, with which a medical diagnosis can be obtained by monitoring vital signs in patients. Such medical devices make it possible to obtain information on people's health status; taking into account the most common signs, such as: blood pressure, heart rate, as well as glucose levels and oxygenation in the blood, among others. However, when it is necessary to make a diagnosis related to mental, ocular and some other health conditions, more sophisticated equipment is required, limiting the scope for access due to its level of specialization and disposition in the medical area. This article proposes the use of pupillometry; as a non-invasive technique, to analyze the response of the photomotor reflex by means of LED flash stimuli in healthy individuals. Through the implementation of an experimental prototype of a low-cost pupillometer, pupillary images of the dominant eye were obtained in 13 people of both genders. This prototype includes a 2 mega-pixel (MP) web camera, a lighting system composed of infrared and RGB led diodes, with which the recording of images in low-light environments is possible, as well as the induction of stimuli for the study of the behavior of the motor reflex, respectively. As results, the design and implementation of a robust algorithm that is capable of estimating the diameters of the pupil is shown, taking into consideration its previous diameters or the variation of its position due to involuntary movements of the subject and recovering samples of information lost due to blinking or partially occluded pupils during image registration. This process has a segmentation performance of 90.5% for all the images acquired. Additionally, with the proposed algorithm, pupillary behavior can be defined through the features of the pupillary diameters before, during and after illumination, obtaining the average impact among the analyzed subjects.

(Received August 8, 2022; accepted August 10, 2023)

Keywords: Pupil light reflex, Pupillometry, Artificial vision system, Image segmentation, LED flash stimuli

1. Introduction

The pupil is a small black hole located in the center of the iris; its function is to regulate the amount of light that enters the eye. Together with the cornea and the lens, the pupil is one of the ocular elements that participate in improving the quality of the image that is formed on the retina. The autonomic nervous system is in charge of controlling involuntary actions, including the size (diameter) of the pupil, its shape and reactivity to light stimuli. The size of the pupil is regulated by two types of muscles: constrictor and dilator, which are innervated by the parasympathetic and sympathetic systems, respectively [1-5]. Generally, in the human eye, the changes that concern the variation of the pupillary diameter are caused by fluctuations in lighting conditions; For example, exposure to the sun at different times of the day, perceiving lights from cars at night, and being in entertainment venues that have strobes. The pupillary light reflex is different for each individual, which is why it is considered a unique and psychological mechanism, which can be used to examine the functioning of the central nervous system, in charge of generating the pupillary response produced before a light stimulus. In recent years the analysis of the pupil has been very important to study the autonomic nervous system and its alterations, such as those that occur in Alzheimer's disease, Parkinson's disease, Diabetes, cognitive load analysis, fatigue, eye tracking, among others [6–12]. Likewise, said analysis has been implemented in mobile technologies and in the implementation of parameters in videogames, allowing to know characteristics evoked through animations, sounds and game modes with low-cost developed equipment [13–18].

In recent years, different authors have carried out studies of pupillary activity for different purposes, using low-cost technologies through the use of conventional cameras, the use of microcontrollers to emit light sequences and the use of infrared light as a source of illumination to improve the quality of the captured images without causing pupillary contraction.

Table 1 presents a summary of the different studies related to pupillometry, which have been carried out using our own designs for the acquisition of pupillary images

and others through the use of commercial research equipment. In this work, a processing and segmentation method is presented for the analysis of images of the pupil, which are obtained by subjecting it to optical stimuli generated with a low-cost digital pupillometer.

Table 1. State of the art of applying the use of pupillary activity analysis

Ref	Device Features	Stimuli features	Proposed or related applications
[19]	- Own Design - Camera (5 MP) - Raspberry Pi-3 model B - Device placement: 17 cm	- Auditory stimulation - Environmental conditions: Normal day light	Variations of emotions in general through auditory stimuli
[20]	- Own design - Logitech Quickcam Pro 5000 (1.3 MP) - Device placement: 50 cm	- On-screen point tracking - Under different sources and types of light	- Eye tracking - Human-machine interface
[21]	- Eyelink 1000 (Commercial device)	- Auditory stimulation	- Qualification of vocal tension and auditory effort
[22]	- Eyelink 1000 (Commercial device)	- Visual tracking - Use of screens	- Attention control
-	- Our device & Method	- LED Stimuli - Dark environment for pupillary reflex to light	

The following section presents the materials and methodology used for the elaboration of the digital pupillometer, where the ethical protocols to be followed, the ergonomic procedure, the acquisition of images, as well as their digital processing are established. The last two sections present the results and conclusions of this work, respectively.

2. Methodology

2.1. Participants

The sample under study consisted of 13 volunteers (6 women and 7 men), healthy young adults aged between 20 and 32 years with no neurological history and no chronic-degenerative diseases. They were students and academics from the Julio Garavito Colombian School of Engineering in Bogotá, Colombia. This study was carried out according to the Declaration of Helsinki, the participants were informed of the action protocol before giving their informed consent.

Questionnaire for the detection of photosensitive epilepsy and ethics endorsement. Given that photosensitive epilepsy is caused by abnormal brain reactions to flashing lights [23], a questionnaire was used to rule out those participants who had ever had a seizure or seizure of epilepsy (under any circumstances: febrile seizure before the age of 5 years, movements, tremors, contractions or spasms, unexplained changes in mental state and / or level of consciousness, unusual movement or behavior when exposed to strobes, video games, flashing lights or the reflection of the sun). Likewise, the study was endorsed by the ethics committee of the Julio Garavito Colombian School of Engineering with a probative document in minutes 004-2018 of the project entitled "Characterization of brain activity under light stimulation". The referred evaluation consisted of an exhaustive review of the experimentation protocol, informed consent, resume, trajectory and experience of the researchers to guarantee the safeguarding of the voluntary population.

2.2. Materials

Digital pupillometer. An optoelectronic device capable of stimulating the pupil by applying light stimuli emitted by light-emitting diodes (LEDs) was designed and built. The manufactured device allows obtaining pupillary diameters, which is achieved through an environment with controlled lighting. In addition to the above, the device can record variations in the diameter of the pupil during stimulation, which allows observing the behavior of the pupillary light reflex. Fig. 1a shows a schematic of the constructed pupillometer. Among the design components are i) a 2 MP webcam located 5 cm from the eye, which is responsible for recording the photomotor reflection, ii) two clusters of infrared LEDs, which allow the pupil to be illuminated inside a cabin dark and iii) a set of LEDs that act as stimulators at different wavelengths (Red = 600nm, Green = 550nm and Blue = 400nm). In fig. 1b the lateral view of the pupillometer is observed. These components are synchronized by means of a graphical interface (Fig.

1c) that controls the COM port of the web camera to be able to visualize the correct posture of the participant's eye. It also manages the resources of the microcontroller (ARDUINO UNO) with its interconnected components (Infrared and LEDs) with the intention of regulating the baseline and stimulation times. The detailed description of the equipment is in the reference [5].

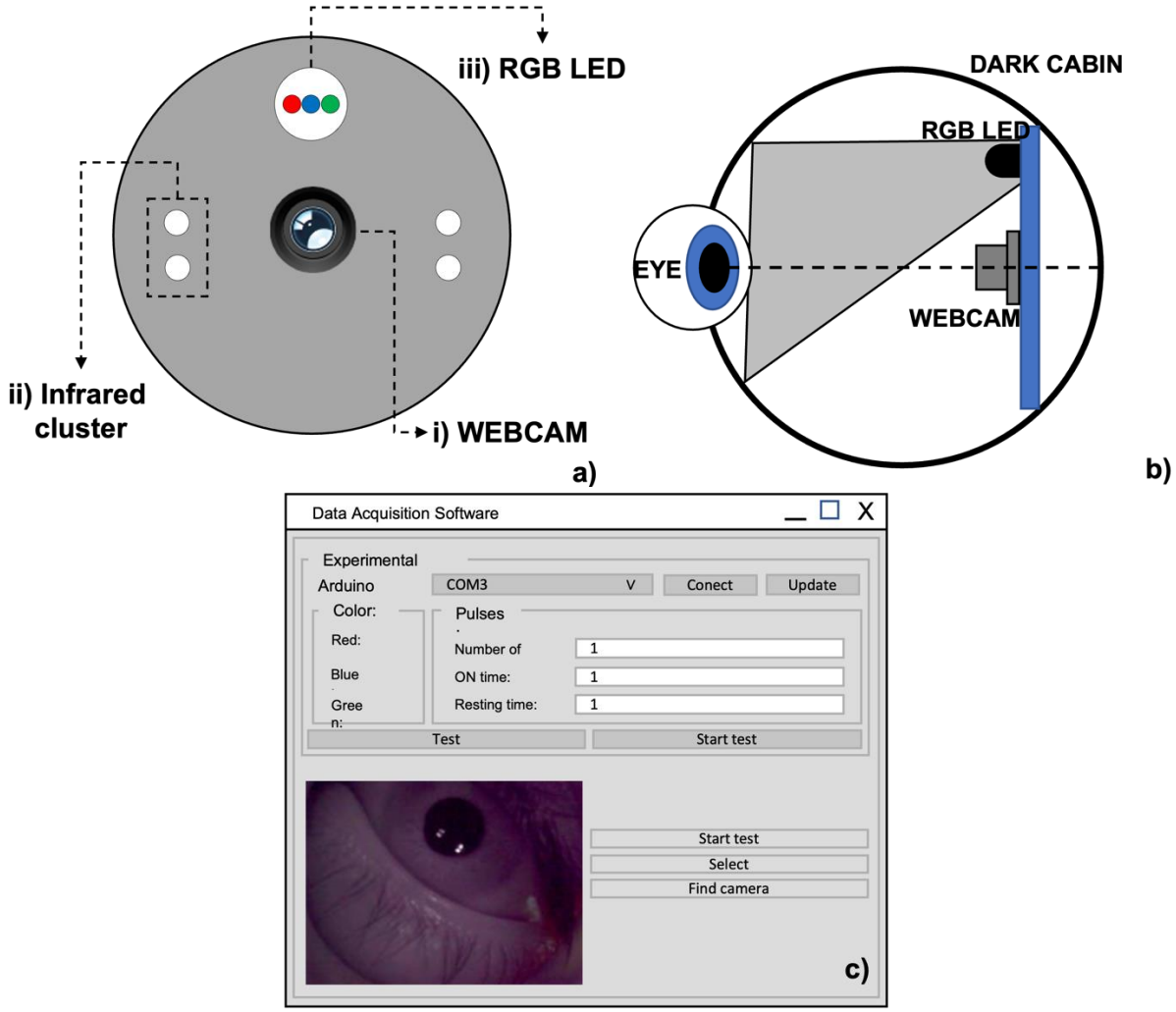

Fig. 1. Pupillometer diagram a) front view b) side view c) data capture module (color online)

Stimulation protocol. For this experiment, the light stimulation source was a red LED (600 nm wavelength), which has been used previously in other works carried out by the research group [1–3] and in other publications related to the subject. in which the use of similar technologies is proposed [24–26]. In order to stabilize the initial size of the pupil, a pre-stimulus (PRE) of 3 seconds was considered, followed by a second of stimulation (ON) and 4 seconds of post-stimulation time (POST). Fig. 2 shows the time and voltage segments applied to LEDs during the experiment.

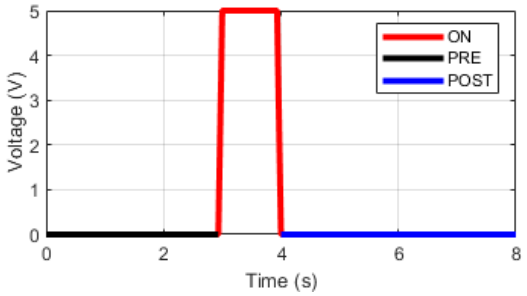

Fig. 2. Time segments of the lighting protocol (color online)

2.3. Procedure

The procedure for this study was as follows:

1. The participants arrived individually at the laboratory and signed an informed consent document, in which the activities to be carried out during the test were explained, as well as, they received indications about the

necessary body posture before the pupilometer, this, to guarantee a test satisfactory. Then, they answered the epilepsy questionnaire, in order to rule out possible seizures in the participants.

2. Then, in a suitable posture, the pupillometer was placed on the participant's dominant eye [10] ; while in the other eye an eye patch was placed in order not to modify the nature of the consensual eye reflex [24], as shown in Fig. 3. The indications prior to carrying out the experiment were the following:

a. Staying with both eyes open for as long as possible before, during and after receiving the flash stimulus.

b. Stare at the center of the device.

c. Do not speak while the video is being acquired or make body movements, with the intention of avoiding other stimuli that could affect the diameter of the pupil. The laboratory environment always remained in the same conditions; ambient lighting lamps turned off and in complete silence, since in studies of analysis of multiple sclerosis and recognition of amblyopic eye they advise taking into account these variables in the environment [27–29].

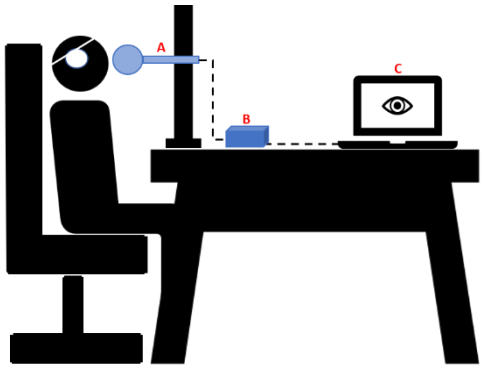

Fig. 3. Experimental position A) pupillometer, B) microcontroller of electronic components, as well as C) graphical interface (color online)

In Fig. 4 the algorithm used for pupillary recognition proposed for this experiment is illustrated.

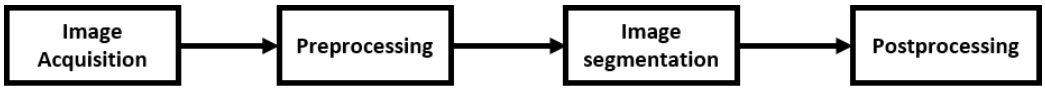

Fig. 4. Pupillometer diagram a) front view b) side view c) Data capture module.

2.4. Image acquisition

All figures must be embedded in the document. When you include the image, make sure to insert the actual image rather than a link to your local computer. As far as possible, use standard PDF conversion tools. Native ‘Save as PDF’ or Adobe Acrobat give best results. It is important that all fonts be embedded/subsetted in the resulting PDF.

2.5. Image processing

2.5.1. Preprocessing

The images were acquired in a uniform lighting environment, with the same device, stimulation, group of people with similar features in age and nationality and the same indications in compliance with the experimental protocol proposed in this method. Once the samples of each of the participants had been acquired, each of the videos was analyzed, in such a way that the following steps are followed (Fig. 5):

a) **Frame load.** In this section each video is analyzed frame by frame.

b) **Channel selection.** For this work, the green and blue color channels were used in the image, since the stimulation by the color of the LED causes saturation in the red channel, it was observed that when analyzing the pictures corresponding to the stimulation time it was not possible obtain similar results to identify the limits of the pupil.

c) **Gray scale conversion.** The Image was transformed into grayscale by means of Matlab's histeq function using an equalization histogram.

d) **Binarization.** With the intention of improving the contrast of the darkest areas where the pupil is positioned, binarization was carried out through Matlab's imbinarize function by means of an adaptive threshold of 0.1 value.

e) **Remove small objects.** Considering that there are different types of patterns formed in the iris by shape or color, a previous process was used to eliminate small objects smaller than 300 px that were around the pupil.

f) **Opening process.** Once having the area of interest with the least possible noise, an opening process was carried out with a structuring element of the disk type with a value of 10. Because the pupil is a circular representation of an object, this process was carried out to correct amorphous shapes in the pupil given by the previous steps.

g) **Fill holes.** Since the previous process denotes two processes (dilation and erosion), in some cases the object of interest could have white pixels and thus make it difficult to segment the pupil. In this way, the white gaps were filled by black color.

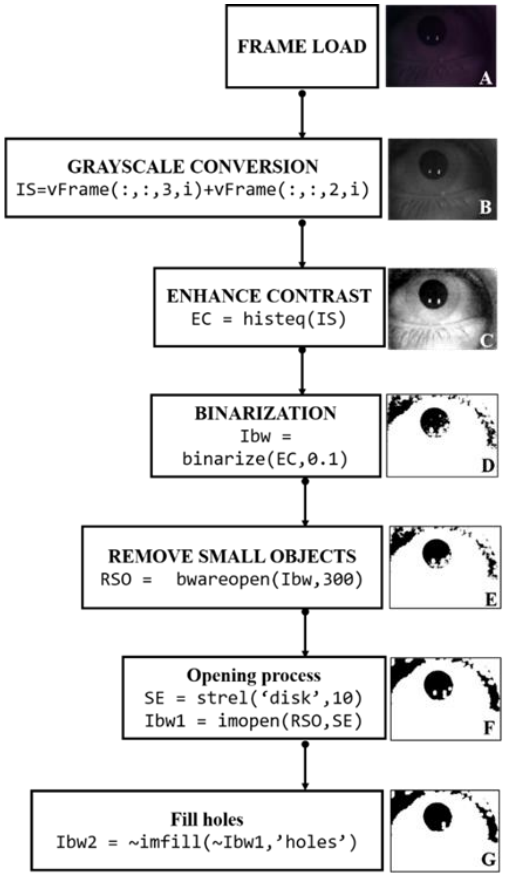

Fig. 5. Preprocessing steps

h) Image segmentation

The selection of images was carried out by discarding those that presented a greater amount of noise from the environment and experimental conditions. Subsequently, the pupil was automatically identified, using the procedure shown in Fig. 6.

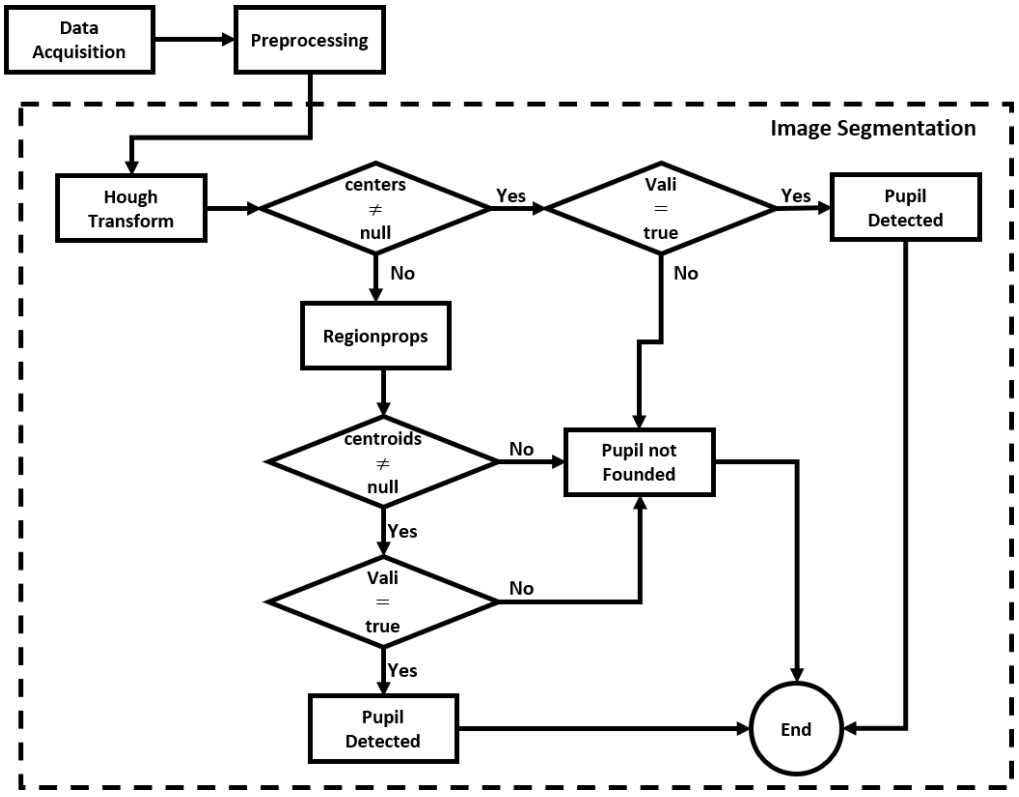

Fig. 6. Image segmentation flowchart

1. Segmentation methods

Two methods of circle segmentation were used in the detection of the pupil, the Hough transform and the use of the Matlab regionprops function. Since we wanted to find the highest number of detections frame by frame, it was decided to use both methods. If the Hough transform [3,30] was not enough to detect circles in the areas of interest, we proceeded to use regionprops [19]. In this way, it was possible to determine that, for the images that presented the pupil slightly occluded, either in the upper or lower part, and even for images where after processing an image with circular morphological features could not be observed, the method segmentation by regionprops yielded better results in the detection process.

2. Validation

Once the objects with a circular shape were detected, we proceeded to validate if the circles found were in accordance with what was expected, this with the intention of minimizing the error when detecting black regions outside the pupil that had semicircular contours and therefore could generate a bad detection. The most frequent cases that were found during the erroneous detection of objects were due to the black areas corresponding to the eyelids, eyelashes and, rarely, to the eyebrows. These erroneous objects appeared recurrently in the image, even in the form of centroids located on the periphery of the same pupil. In these cases, the Hough and regionprops methods were able to superimpose two or more circles in the area of interest of the pupil. In Fig. 7 you can see these shapes and objects that in certain regions contain semicircular shapes, in red those belonging to the eyelid, eyebrow and eyelashes are shown and in blue areas of the pupil, these were sometimes detected as circular objects.

Fig. 7. Semi-circular areas (color online)

The above was resolved by means of a validation stage after detection with one of the two previously mentioned segmentation methods:

Variation in size. In the knowledge that the pupil in healthy people does not change abruptly, a tolerance variable was established for its size, which would allow us to identify if a previous pupil diameter, compared to the current one, does not belong to the normal pupillary behavior under observation. Based on multiple tests in the validation phase of the algorithm, a tolerance margin of 30% was established in the variation of its size with respect to the previous diameter, since with this value it was possible to discern the correct and incorrect diameters.

Movement variation in X and Y axes. This validation allowed discarding objects located around the image. Given that each participant followed the indication to stare at the center of the pupillometer, those areas far from the center of the image could be ruled out by means of another variable that validated the position of the diameters found with respect to their location on the axes (x and y). This provided some flexibility in the natural movement of the eye caused by the flash. In the stimulation, a value greater than and equal to 70% of variation was assigned in order to obtain a valid measurement without considering objects belonging to eyelids, eyebrows and eyelashes. Thus, both validations were used after the detection of each perimeter of the pupils, after which the correct radius were stored in a vector and the incorrect radius were marked as NaN (not a number).

2.5.2. Post-processing

For those images in which it was not possible to segment the pupil by calculating the centroid corresponding to the radius, the following steps were applied as post-processing:

Interpolation: In this step, a process of recovering the radius in which their estimation was not possible in a certain frame was carried out and that were possibly caused by partial or total occlusions of the eye and / or the segmentation functions. To retrieve the related information, a cubic interpolation by sections with shape preservation was used.

Filtering: A grade 3 medians filter was used to smooth the peaks in the images and better observe the pupillary behavior to light stimuli [31,32].

Simulation process: To test if the interpolation was consistent, a simulation was performed where a sigmoid function was described, which in its nature is very similar to the pupillary response under light stimuli. To test performance in this process, a Gaussian white noise function was applied; In addition, records of the signal were randomly eliminated, these with a maximum number of 33 records, which were taken from the sample with the highest number of losses in the measurement of the pupillary radius. In Fig. 8 the different simulation steps are shown: a) sigmoid signal generation b) Gaussian white noise and elimination of random records c) interpolation and filtering stage d) comparison of the expected signal and the simulated signal.

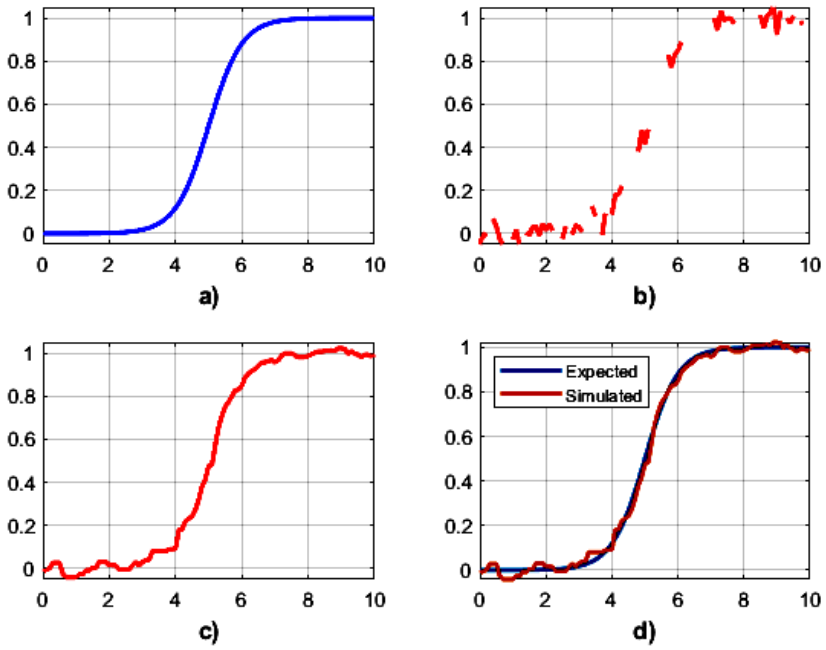

Fig. 8. Sigmoid signal simulation processes (color online)

Analysis of the average pupillary response

Considering the average reaction time of the pupil to a visual stimulus, which in humans is 250 ms [33], the average diameters were calculated for each time of the experiment (PRE, ON and POST). Likewise, the impact of the stimulus was calculated using the following formula (1).

$$I = \frac{POST}{PRE}. \quad (1)$$

With the intention of observing the relative change after the presented stimulus. The range of the PRE, ON, and POST stage are respectively 1-49 frames, 50-65 frames, and 66-120 frames.

3. Results

This section shows interesting features in the use of the algorithm for the analysis of the pupillary response in the recognition and segmentation of the pupillary radius, as well as the average response obtained through each of the samples in each of the 13 participants. In this study, the acquisition of images of the pupil was performed using a low-cost device with inferior features, compared to clinical equipment and experimental designs. The use of a 2 MP webcam, an infrared lighting system with conventional infrared diodes and a stimulation system of conventional LEDs and control by means of the Arduino UNO microcontroller can be highlighted.

On the other hand, the robustness and usefulness of the segmentation algorithm stands out, in which images of the participants with their eyes completely open, partially occluded and blinking, among others, were recorded. In Fig. 9 an example of a participant who correctly attended the previously received indications is shown, obtaining an absolute segmentation of the pupillary diameter. (The paragraphs in the figure correspond to the steps of image pre-processing and segmentation).

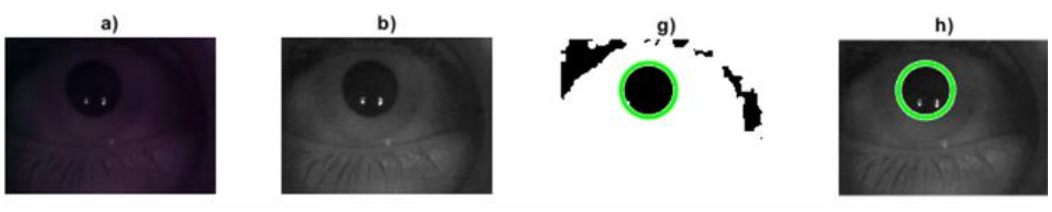

Fig. 9. Perfectly open eye box (color online)

Likewise, the combination of segmentation techniques (Hough transform and Matlab regionprops) allowed us to analyze not only perfectly well-formed circles but also to recognize the nature of objects with a greater circular appearance in certain parts of the common areas of the pupil and the use of morphological operators that complemented said regions in the form of the disk structuring element. In Fig. 10 it can be seen a sample for

the case of a pupil partially occluded by the eyelid, however, this has been successfully detected with the proposed method.

Fig. 10. Eye frame with partially occluded pupil (color online)

In other cases, derived from small regions that remain even after the processing stage, white pixels that are preserved and circular edges present in the pupil, there were cases where more than one centroid corresponding to other foreign circular areas were detected. In these cases, the validations of pupillary size and movement percentages allowed the selection of the centroid related to the previous tables. In Fig. 11 the detection of 2 circles is shown and the algorithm detects which of them is the one that has the greatest relationship with the previous pupillary behavior.

Fig. 11. Multiple centroids found (color online)

Once all the samples of the participants had been processed, the average pupillary response was calculated, previously a normalization process was carried out between 0 and 1 with the intention of better observing the individual behavior and being able to average each of the samples. In Fig. 12 it is possible to observe the processes of a) acquired original signals, b) interpolated signals, c) filtered signals, d) normalized signals, e) calculation of the average response and f) average response and the time segment of the stimulus of light. In this way, we can observe visually similar behaviors in the pupillary reaction by means of LED Flash-type light patterns, which is very important for the simplicity of the equipment used and the improvements added compared to previous works in the use of the digital pupillometer.

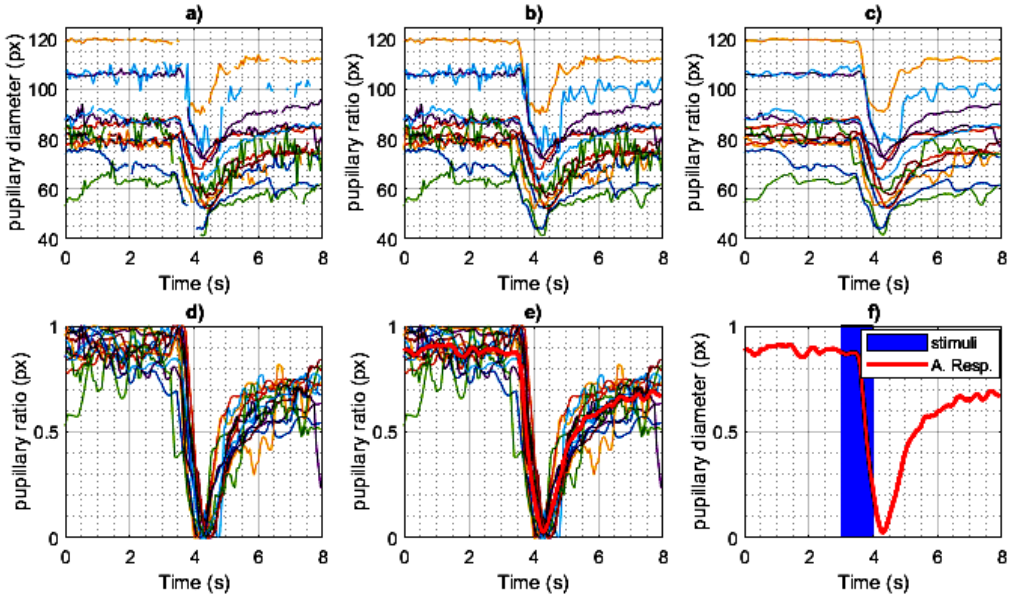

Fig. 12. Post-processing steps and average pupillary response (color online)

Table 2 shows the main features of the participants, the non-segmented samples, those recovered in the processing stage, the average diameters in pixels corresponding to each moment of the experiment (PRE, ON and POST) for each of the participants and the impact of the visual stimulus.

Regarding the performance for the detection of pupillary diameters, a 90.5% effectiveness was obtained, taking into account complicated scenarios with the physiological variation of the eyelids and unintentional blinks at the time of carrying out the experiment. On the other hand, a greater loss is registered with 33 samples not segmented in participant 7 and an average of 9.5% of the sample in general. Subsequently, from these non-segmented samples, 98.6% is recovered through the post-processing stage, thus having only 2 non-recovered samples (1.4%). Based on the averages of the pupillary response at each time and the visual impact, a trend between values of 0.8 and 0.9 can be observed for the entire sample, likewise the diameters prior to the stimulus in most cases have a greater magnitude with regarding the diameters of the response during and after the stimulus. For the impact (I), an average of 0.9 is found in particular, this denotes the variation obtained in the diameter of the pupil after undergoing a brief stimulus, however, this maintains a pattern that fits in a population way.

Table 2. Imaging Ranges for Average Pupillary Response, no segmented samples (NSS), Recovered Samples (RS), Impact(I)

	Sex	Edge	NSS	RS	Pre	On	Post	I
1	F	23	5	5	80	68	67	0.8
2	M	24	1	1	86	78	82	0.9
3	M	22	14	14	120	105	109	0.9
4	F	21	2	2	106	95	88	0.8
5	M	22	8	8	62	55	56	0.9
6	M	24	28	28	106	96	96	0.9
7	M	22	33	33	81	74	71	0.9
8	F	21	5	5	71	55	59	0.8
9	F	22	1	1	79	73	70	0.9
10	M	32	27	25	79	65	66	0.8
11	M	22	4	4	88	81	82	0.9
12	F	20	18	18	83	67	73	0.9
13	F	22	2	2	89	78	79	0.9

4. Conclusions and future work

In this work we have investigated the dilation and constriction of the pupil using a low-cost pupillometer and the implementation of a recognition algorithm. The results obtained show that the use of morphological operators, filtering and dynamic segmentation, provide adequate image processing. The introduction of validation parameters ensures reliable measurements that adequately describe pupillary behavior. The segmentation process allows to rescue samples that in principle could be discarded or canceled due to factors associated with the experiment or conditions of the analyzed eye (too large pupils, drooping eyelids, and micro-blinks). In the same way, the performance range is exposed, which compared to most of the studies cited, does not show a concise precision and it is also possible to recover samples. Future work seeks to find the relationship between the function of the photomotor reflex and the brain activity derived from stimulation by means of LED light, as well as to propose stimulation protocols that allow offering alternatives for the analysis of flash-type evoked visual potentials to offer diagnostic techniques with greater portability, lower costs of maintenance of equipment, processing, and multiple applications with the interaction of brain machine interfaces.

Inexpensive pupilometers offer advantages over high-end devices in terms of affordability, accessibility, and portability.

Lower cost allows for greater reach, especially in resource-limited settings such as community clinics and hospitals.

Its portable design and simplicity make it easy to use in remote areas, which is beneficial for the early detection and diagnosis of eye diseases in places with limited access to medical care. Additionally, today's inexpensive pupillometers incorporate advanced digital technology, including high-resolution cameras and image processing software, ensuring accurate and consistent measurements.

The implementation of image recognition and processing algorithms further improves the accuracy and reliability of measurements compared to high-end devices.

References

[1] S. U. López, D. A. Gutiérrez Hernández, V. Zamudio, L. E. Mancilla Espinoza, J. G. Cárdenas Solís, M. T. Galvan González, J. C. Estrada, 2017 International Conference on Electronics, Communications and Computers (CONIELECOMP), IEEE, 1 (2017).

[2] M. T. Galvan González, D. A. Gutiérrez Hernández, V. Zamudio, C. Lino, J. G. Cárdenas Solís, S. U. López, E. Guevara, 2017 International Conference on Electronics, Communications and Computers (CONIELECOMP), IEEE, 1 (2017).

[3] J. G. Cardenas Solis, D. A. Gutierrez Hernandez, Edgar Guevara, R. Santiago-Montero, M. T. Galvan Gonzalez, S. U. Lopez, R. Rodriguez Montero, J. M. Carpio, Advances in Computing **7**(1), 1 (2017).

[4] Xiaofei Fan, Gang Yao, IEEE Trans Biomed Eng. **58**(1), 36 (2011).

[5] D. A. G. Hernández, J. A. Aranda Ruiz, Int. J. Sci. Res. **2**(4), 85 (2012).

[6] L. Y.-L. Chang, J. Turuwhenua, T. Y. Qu,

J. M. Black, M. L. Acosta, Frontiers in Integrative Neuroscience **11**(6), PMC5339232 (2017).
[7] Y. Wang, A. A. Zekveld, D. Wendt, T. Lunner, G. Naylor, S. E. Kramer, PLoS One **13**(6), e0197739 (2018).
[8] A. Bianchetti, L. I. Perez, S. A. Comastri, Proceedings of SPIE – The International Society for Optical Engineering, 8785 (2013).
[9] A. G. Lerner, A. Bernabe-Ortiz, R. Ticse, A. Hernandez, Y. Huaylinos, M. E. Pinto, G. Malaga, W. Checkley, R. H. Gilman, J. J. Miranda, Diabetic Medicine **32**(11), 1470 (2015).
[10] A. J. Oh, G. Amore, W. Sultan, S. Asanad, J. C. Park, M. Romagnoli, C. La Morgia, R. Karanjia, M. G. Harrington, A. A. Sadun, PLoS One **14**(12), e0226197 (2019).
[11] T. Tabashum, A. Zaffer, R. Yousefzai, K. Colleta, M. B. Jost, Y. S. Park, J. Chawla, B. Gaynes, M. V. Albert, T. Xiao, Frontiers in Medicine **8**, 645293 (2021).
[12] W.-L. Ou, T.-L. Kuo, C.-C. Chang, C.-P. Fan, Applied Sciences **11**(2), 851 (2021).
[13] J. Kotani, H. Nakao, I. Yamada, A. Miyawaki, N. Mambo, Y. Ono, Front Med. **8**, 598791 (2021).
[14] C. Barry, J. de Souza, Y. Xuan, J. Holden, E. Granholm, E. J. Wang, in CHI Conference on Human Factors in Computing Systems, New York, NY, USA: ACM, Apr., 1 (2022).
[15] L. Cardinali, S. Roatta, R. Pertusio, M. Testa, C. Moglia, Electronics **11**(22), 11223713 (2022).
[16] L. B. McGrath, J. Eaton, I. J. Abecassis, A. Maxin, C. Kelly, R. M. Chesnut, M. R. Levitt, Frontiers in Neuroscience **16**, 893711 (2022).
[17] R. E. McKay, M. A. Kohn, E. S. Schwartz, M. D. Larson, Concussion **5**(4), 0016 (2020).
[18] J. J. McAnany, B. M. Smith, A. Garland, S. L. Kagen, Optometry and Vision Science **95**(10), 953 (2018).
[19] S. Rafique, N. Kanwal, I. Karamat, M. N. Asghar, M. Fleury, IEEE Access **9**, 5354 (2021).
[20] K.-F. Lee, Y.-L. Chen, C.-W. Jen, K.-Y. Chin, C.-W. Hung, C.-B. Wen, Journal of Low Frequency Noise, Vibration and Active Control **40**(1), 18 (2021).
[21] M. Farahani, V. Parsa, B. Herrmann, M. Kadem, I. Johnsrude, P. C. Doyle, Applied Sciences **10**(17), 5907 (2020).
[22] J. L. Irons, M. Jeon, A. B. Leber, PLoS One **12**(12), e0188787 (2017).
[23] G. Strigaro, B. Gori, C. Varrasi, T. Fleetwood, G. Cantello, R. Cantello, Epilepsy Res. **172**, 106597 (2021).
[24] M. Bernabei, L. Rovati, L. Peretto, R. Tinarelli, 2015 IEEE International Instrumentation and Measurement Technology Conference (I2MTC) Proceedings, IEEE, May, 1634 (2015).
[25] S. Y. Moon, J. P. Lee, J. H. Bae, T. S. Lee, Biomed. Eng. Lett. **5**(1), 29 (2015).
[26] P. Adhikari, A. J. Zele, B. Feigl, Investigative Opthalmology and Visual Science **56**(6), 3838 (2015).
[27] N. van der Stoep, M. J. van der Smagt, C. Notaro, Z. Spock, M. Naber, Sci. Rep. **11**(1), 707 (2021).
[28] G. Bitirgen, Z. Akpinar, H. B. Turk, R. A. Malik, Transl. Vis. Sci. Technol. **10**(4), 30 (2021).
[29] G. Bitirgen, M. Daraghma, A. Özkağnıcı, Turk J. Ophthalmol. **49**(6), 310 (2019).
[30] A. Amodio, M. Ermidoro, D. Maggi, S. M. Savaresi, in 2018 European Control Conference (ECC), IEEE, Jun., 2691 (2018).
[31] W. Fuhl, T. C. Santini, T. Kübler, E. Kasneci, Proceedings of the Ninth Biennial ACM Symposium on Eye Tracking Research & Applications, New York, USA, 123 (2016).
[32] H. K. Wong, J. Epps, S. Chen, IEEE Trans. Cogn. Dev. Syst. **11**(4), 560 (2019).
[33] P. D. R. Gamlin, H. Zhang, A. Harlow, J. L. Barbur, Vision Res. **38**(21), 3353 (1998).

*Corresponding author: francisco.casillas@academicos.udg.mx